



Improving gold recovery from a refractory ore via Na₂SO₄ assisted roasting and alkaline Na₂S leaching

Xiaoliang Liu^{a,b}, Qian Li^{a,*}, Yan Zhang^{a,b}, Tao Jiang^a, Yongbin Yang^a, Bin Xu^a, Yinghe He^{b,*}

^a School of Minerals Processing and Bioengineering, Central South University, Changsha, Hunan 410083, PR China

^b College of Science and Engineering, James Cook University, Townsville, Queensland 4811, Australia

ARTICLE INFO

Keywords:

Refractory gold ore
Na₂SO₄ assisted roasting
Thermodynamic analysis
Alkaline Na₂S leaching

ABSTRACT

Gold recovery from refractory gold ores with controlled roasting remained well below 80%. Na₂SO₄ was added in an O₂-enriched single stage roasting of a refractory gold ore to improve its gold recovery. Changes in physicochemical properties of the calcines suggested that this reduced the sintering as well as facilitated the formation of pores and a water soluble phase within the calcine. Thermodynamic analysis and leaching results demonstrated that Na₂S solutions could effectively remove Sb species from the calcine. An extraction process that includes Na₂SO₄ assisted roasting and alkaline Na₂S leaching is shown to be able to achieve a gold recovery of over 95% from the refractory ore.

1. Introduction

In our previous research (Liu et al., unpublished results, 2018), an optimised O₂-enriched single-stage roasting achieved the simultaneous removal of S, As and C from a refractory gold ore, and an improved gold recovery of 72.5%. However, it is still unsatisfactory. Analyses of calcines from the controlled roasting suggested that the main causes for the low recovery were likely to be the secondary encapsulation of gold particles caused by the local high temperature during roasting and the existence of Sb in the calcine.

Sintering often occurs during roasting, particularly under an O₂-enriched atmosphere due to the enormous amount of heat released from the oxidation of S and C (Li et al., 2017). It could result in secondary encapsulation of gold in the calcine that prevents its exposure to the extraction medium and therefore ultimate extraction.

In refractory gold ores, Sb exists mainly as stibnite (Sb₂S₃) and is difficult to remove together with S, As and C through roasting due to the conflicting requirements (Padilla et al., 2010, 2014). In contrast with an O₂-enriched (40 vol%) roasting at 650 °C for the simultaneous removal of S, As and C (Liu et al., unpublished results, 2018), low oxygen concentrations (around 1–5 vol%) and high temperatures (> 900 °C) are required to efficiently volatilize stibnite to antimony trioxide (Sb₂O₃); otherwise, Sb would remain in the calcine in the form of less volatile Sb₂O₃ and/or nonvolatile Sb₂O₄ (or SbO₂) (Kyle et al., 2012; Padilla et al., 2010, 2014; Živkovića et al., 2002). The presence of Sb in gold ores > 0.5 wt% has been found to severely hamper or

prevent cyanidation since Sb can consume oxygen and cyanide and/or passivate gold particles by forming oxyanions, thioanions and/or precipitates (Kyle et al., 2012; Thomas and Cole, 2016).

In order to attain an acceptable level of gold recovery, the sintering phenomenon must be prevented during roasting, and the Sb must be removed before cyanidation. Additives are often utilised to modify the roasting process for a range of ores. Sodium sulphate (Na₂SO₄) has been reported to be an effective additive in the oxidative roasting of sulphide ores to improve the extraction of valuable metals such as Cu, Co and Ni (Guo et al., 2009; Li et al., 2018; Prasad and Pandey, 1998; Rao et al., 2001). This is likely attributed to the relief of sintering and/or the formation of a porous structure for calcines during the Na₂SO₄ assisted roasting (Guo et al., 2009; Li et al., 2018). The beneficial effects of Na₂SO₄, however, are seldom applied to the roasting of refractory gold ores. Alkaline sulphide leaching at relatively high temperatures (> 70 °C) has proven to be suitable for removing Sb from antimonial sulphide gold ores/concentrates (Awe and Sandström, 2010; Baláz and Achimovičová, 2006; Baláz et al., 2000; Celep et al., 2011; Gök, 2014; Li et al., 2011; Liu et al., unpublished results, 2018; Raschman and Sminčáková, 2012; Sminčáková and Raschman, 2011; Ubaldini et al., 2000; Zeng et al., 2018). In addition, the oxides of Sb such as Sb₂O₃ can also be dissolved in alkaline solutions (King, 2005).

This paper reports our attempt to improve the gold recovery from refractory gold ore. Na₂SO₄ is added to further optimise the O₂-enriched single stage roasting. An alkaline sulphide leaching step is also added to remove Sb. Thermodynamic analyses are used to establish possible mechanisms for the experimentally observed improvements.

* Corresponding authors.

E-mail addresses: csuliqian208018@csu.edu.cn (Q. Li), yinghe.he@jcu.edu.au (Y. He).

<https://doi.org/10.1016/j.hydromet.2019.02.008>

Received 3 November 2018; Received in revised form 14 January 2019; Accepted 15 February 2019

Available online 17 February 2019

0304-386X/ © 2019 Elsevier B.V. All rights reserved.

Table 1
Chemical composition of the gold ore/(wt%).

Au ^a	SiO ₂	CaO	MgO	Al ₂ O ₃	As	Fe	S	Sb	C	K ₂ O
18.05	27.68	4.26	5.86	2.19	1.62	19.60	20.60	1.31	6.95	2.10

^a Unit g/t.

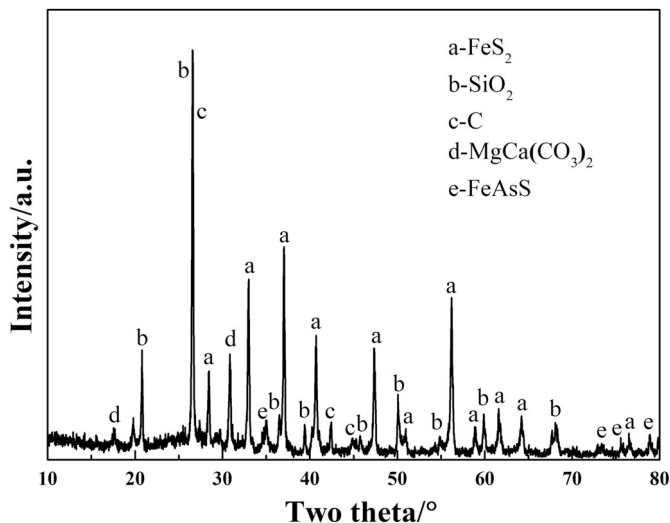


Fig. 1. XRD spectrogram of the gold ore.

2. Thermodynamic calculations

HSC Chemistry 6.0 for Windows (Roine, 2006) based on STBCAL (Haug, 1989; Haug and Cuentas, 1989) was used to construct the Eh–pH diagram for Sb–S–H₂O system. The available thermodynamic data are listed in Appendix A. Under a given solution condition of

Table 2
Chemical phases of As, S, C, Sb and Au in the gold ore/(wt%).

Phase of As	Elemental arsenic	Arsenic oxide	Arsenic sulphide	Arsenate	Arsenopyrite	Total
Content	0.025	0.002	0.231	0.241	1.12	1.62
Distribution	1.54	0.12	14.27	14.89	69.18	100.00
Phase of S	Sulphide	Sulphate	Elemental sulphur	Total		
Content	20.10	0.15	0.35	20.60		
Distribution	97.57	0.73	1.70	100.00		
Phase of C	Carbonate	Organic carbon	Elemental carbon	Total		
Content	1.71	0.50	4.74	6.95		
Distribution	24.60	7.20	68.20	100.00		
Phase of Sb	Antimony oxide	Antimony sulphide	Antimonate	Total		
Content	0.077	1.182	0.051	1.31		
Distribution	5.88	90.23	3.89	100.00		
Phase of Au	Leachable gold ^b	Encapsulated in arsenopyrite	Encapsulated in sulphides	Encapsulated in oxides	Encapsulated in silicates	Total
Content ^a	0.31	12.07	3.69	1.87	0.11	18.05
Distribution	1.72	66.87	20.44	10.36	0.61	100.00

^a Unit g/t.

^b The amount of leachable gold in the ore was determined by direct cyanidation of the ore.

temperature, pressure, and concentrations of Sb and S, the predominance areas of Sb species in the system can be shown on a relevant scale in an Eh(vs. SHE)–pH diagram.

The speciation diagrams for Sb species were constructed using Medusa-Hydra chemical equilibrium software for Windows (Puigdomenech, 2004) based on an algorithm of SOLGASWATER (Eriksson, 1979). The thermodynamic data and relevant species are from the hydrochemical log *K* database of the software. Given the system status of Eh (vs. SHE), pH, and total concentrations of Sb and S, the concentrations (M) or mole fractions (%) of all Sb species co-existing in an equilibrium state can be estimated from their equilibrium constants (log *K*).

3. Experimental

3.1. Materials and reagents

The refractory gold ore was a concentrate with over 80 wt% of the particles smaller than 74 μm in size. As shown in Table 1, it contained Au 18.05 g/t. The weight percentages of the impurities of concern are: As 1.62%, S 20.76%, C 6.95% and Sb 1.31%, respectively. The total content of SiO₂, CaO, MgO and Al₂O₃ reached ~40%, which can cause sintering and agglomeration under high temperatures (Li et al., 2017). The XRD spectrogram presented in Fig. 1 indicates that the main mineral phases of the ore consisted of pyrite, arsenopyrite, carbon, quartz and dolomite. No Sb phase was detected by XRD due mainly to its low content (1.31%). A widely accepted proprietary procedure (detailed in Section 3.3) was used to quantify the chemical phases of the ore. As listed in Table 2, 69.18% of the As occurred as arsenopyrite, 97.57% of the S as sulphide (mainly pyrite), and 68.2% of the C as elemental carbon. Most (90.23%) of the Sb occurred as antimony sulphide (mainly stibnite). In terms of the chemical phase of gold, only 1.72% of gold was leachable while 66.87% was encapsulated in arsenopyrite, 20.44% in sulphides (mainly pyrite), and 10.36% in oxides (mainly iron oxides).

The chemicals used in the roasting and leaching experiments including sodium sulphate, sodium sulphide, sodium hydroxide, sulphuric acid and sodium cyanide were all AR grade. The purity of both

the nitrogen and oxygen was over 99.5%. De-ionised water was used throughout all experiments.

3.2. Experiment methods

The experimental set-up for roasting is schematically shown in Fig. 2. The roasting of the gold ore with a particle size of over 80 wt% $-74\ \mu\text{m}$ was conducted in a quartz tube in a horizontal tube furnace. Prior to the roasting, the temperature was elevated to $650\ ^\circ\text{C}$ ($923\ \text{K}$). Nitrogen was then passed to flush the air out from the tube. The roasting atmosphere was controlled by adjusting the volume flowrate ratio between oxygen and nitrogen with a total flowrate of $1\ \text{L}/\text{min}$. After the tube was completely flushed with O_2 of 40 vol%, 50 g of the gold ore mixed with a desired amount of Na_2SO_4 loaded in a porcelain boat was pushed into the quartz tube directly below the thermocouple. Simultaneously, a vacuum pump operated during the whole roasting process to ensure a very slight vacuum in the tube. The exhaust gas was scrubbed with two bottles of saturated NaOH solution. After roasting 30 min, the calcine was taken out of the tube furnace and naturally cooled in air, and collected for further tests or chemical analyses.

Water washing, alkaline Na_2S leaching, and cyanide leaching of the concentrate or calcine were all carried out in a 1-L jacketed glass reactor equipped with a constant temperature bath and an overhead mechanical stirrer (IKA EURO-STPCUS25). The water washing conditions were liquid-solid mass ratio 3:1, temperature $25(\pm 0.5)\ ^\circ\text{C}$, stirring speed 300 rpm, time 30 min. Before leaching with alkaline Na_2S and/or cyanide solutions, the concentrate or calcine was wet-milled in a ball mill to be over 80 wt% $-45\ \mu\text{m}$. The alkaline Na_2S leaching conditions were liquid-solid mass ratio 3:1, temperature $80\ ^\circ\text{C}$, stirring speed 300 rpm, Na_2S 0–15 g/L, NaOH 20 g/L and leaching time 1 h. It should be noted that the water washing of the calcine also occurs during the wet grinding and/or alkaline Na_2S leaching process. The cyanidation conditions were liquid-solid mass ratio 2.5:1, temperature $25(\pm 0.5)\ ^\circ\text{C}$, stirring speed 600 rpm, NaCN 0.3 wt%, leaching time 36 h, and pH 11, adjusted by controlled addition of 1.0 M NaOH solution. Filtration of the solid residues from the water washing, alkaline Na_2S leaching and/or cyanidation tests was carried out with a vacuum filter with copious de-ionised water. The respective filter cakes were then dried in a vacuum oven and collected separately for subsequent tests or assays.

3.3. Analytical methods

The contents of S and C in solids were determined by a high frequency IR carbon and sulphur analyser (HW2000B, Wuxi Yingzhicheng) while the other elements in solids were assayed through acid digestion and an atomic absorption spectrometer (AA-6800, Shimadzu). The concentration of Au in solution was measured by ICP-AES (PS-6, Baird). The morphology and mineralogical phases of the ore,

calcine and residue were determined using SEM coupled with EDS (JSM-6360LV, JEOL) and an X-ray diffractometer (D/Max 2500, Rigaku), respectively. The size distribution of the particles was determined by wet-screening using sieves of different meshes. The specific surface area of the particles was measured with a BET surface area analyser (Model F-Sorb 2400, Beijing Jinaipu Technical Apparatus Co., Ltd.). The TG/DTG/DSC curves of the gold ore were determined with a thermogravimetry (TG/DTG) and differential scanning calorimetry (DSC) instrument (NETZSCH STA 449C, NETZSCH Group).

The chemical phases of As, S, C, Sb and Au presented in Table 2 were determined with a proprietary but widely accepted analytical procedure developed by Changsha Research Institute of Mining and Metallurgy Co., Ltd. Fundamentally, the phases of elements were determined from a series of treatments of cyanidation, roasting, and leaching with NaOH and various acids including HNO_3 , aqua regia, HF and HClO_4 . More details can be found in Xu et al. (2016).

4. Results and discussion

4.1. Reduction of sintering during roasting

4.1.1. Effect of Na_2SO_4 addition on physicochemical properties of calcines

Fig. 3 presents the SEM images of calcines that shows the effects of Na_2SO_4 addition in roasting and water washing on the morphologies of the calcines. When no Na_2SO_4 was added, Fig. 3(b) shows the obtained calcine particles have some signs of sintering on the surface. While not shown, the size, morphology and surface of these calcines hardly changed from water washing, implying negligible presence of water-soluble phase in the calcines. Comparison of Fig. 3(d) with (b), and Fig. 3(c) with (a), suggests that the presence of Na_2SO_4 during roasting caused a more severe sintering during roasting, resulting in a larger calcine particle size as well as partial melting on the surface of the particles. However, the phase that partially melted and sintered the particles together is water soluble as evidenced by the smaller calcine particle size and more porous surface seen in Fig. 3(e) and (f) after the water wash. The differences are quantified by comparing the particle size distribution and specific surface area between Samples S_1 and S_3 . The results are presented in Table 3 where Na_2SO_4 assisted roasting followed by water washing have resulted in the formation of smaller and much more porous particles with a specific surface area increase from $2084\ \text{cm}^2/\text{g}$ to $3249\ \text{cm}^2/\text{g}$. The EDS data for S_2 and S_3 listed in Table 4 suggest that the above changes are likely caused by the formation of some Na- and S-containing phases during the Na_2SO_4 assisted roasting. The phases must have a low melting point to cause the visible sintering, and must be water soluble that their quantity in the calcine S_3 is much reduced after the water wash.

To determine the phases, XRD surveys were performed on the calcines $S_1 - S_3$ and their spectrograms are shown in Fig. 4. Two major

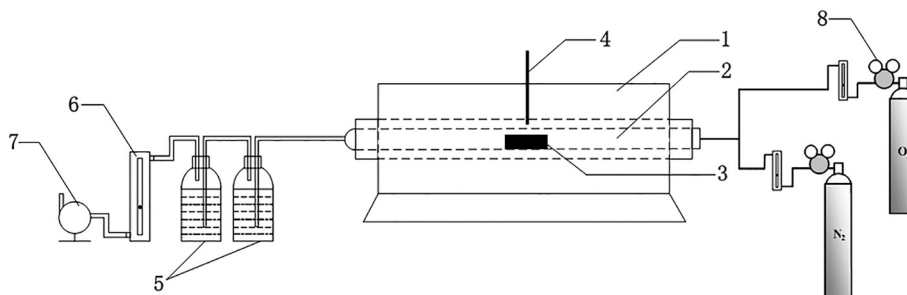


Fig. 2. Schematic diagram of the experimental device for oxidative roasting. 1-horizontal tube furnace; 2-quartz tube; 3-sample in a ceramic boat; 4-thermocouple; 5-exhaust gas scrubber; 6-rotameter; 7-vacuum pump; 8-pressure regulator.

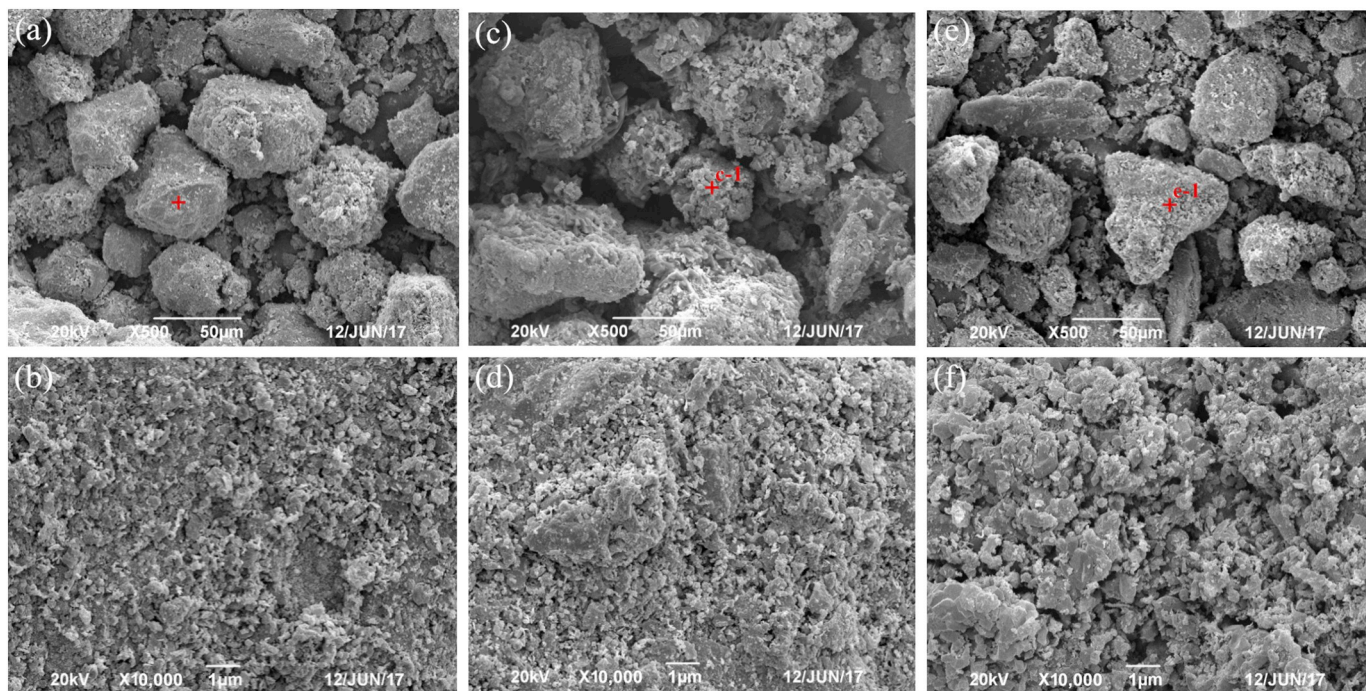


Fig. 3. SEM images for the calcines of (a)/(b) S₁, (c)/(d) S₂, and (e)/(f) S₃. Conditions: S₁: roasting without Na₂SO₄ or water washing; S₂: roasting with 3 wt% Na₂SO₄ and no water washing; S₃: roasting with 3 wt% Na₂SO₄ and water washing.

Table 3
Particle size distribution and specific surface area of the calcines of S₁ and S₃.

Calcine	Size fraction distribution/(wt%)				Specific surface area/(cm ² /g)
	+74 μm	37–74 μm	–37 μm	Total	
S ₁	46.64	24.78	28.58	100	2084
S ₃	35.92	20.81	43.27	100	3249

Table 4
EDS data for the calcines of S₂ and S₃/(wt%).

Spots ^a	Na	Mg	Al	Si	S	K	Ca	Ti	Fe	O
c-1 (in S ₂)	7.42	1.33	2.36	5.89	14.63	0.63	1.91	0.36	36.7	28.77
e-1 (in S ₃)	0.8	2.59	2.75	8.36	4.82	0.87	3.48	0.46	42.17	33.68

^a Analysed spots are in correlation with those in Fig. 3.

differences should be noted. Firstly, the peak for a typical sintering phase of (Ca,Mg)Si₂O₆ is present in S₁; its intensity and areas are much reduced in S₂ or S₃. Secondly, Na₂SO₄ peaks appeared in S₂ but not in S₁ or S₃.

As our previous research results established that the presence of (Ca,Mg)Si₂O₆ was a sign of sintering during roasting (Li et al., 2017). Visually, Fig. 3 shows the extent of sintering is much more prominent in S₂ than in S₁. However, there is no (Ca,Mg)Si₂O₆ in S₂. Instead, Na₂SO₄ is present. With a melting point of 884 °C, it is unlikely for Na₂SO₄ to cause significant sintering as it is much higher than the roasting temperature of 650 °C. This suggests that an intermediate low-melting phase must have formed during roasting but eventually disappeared at the completion of roasting.

Many studies suggest that Na₂SO₄ can react with SO_x (i.e., SO₂ and SO₃) and O₂ to form sodium purosulphate (Na₂S₂O₇) as shown in Eqs. (1)–(3) with Eq. (3) being the total reaction of Eqs. (1) and (2) (Lam,

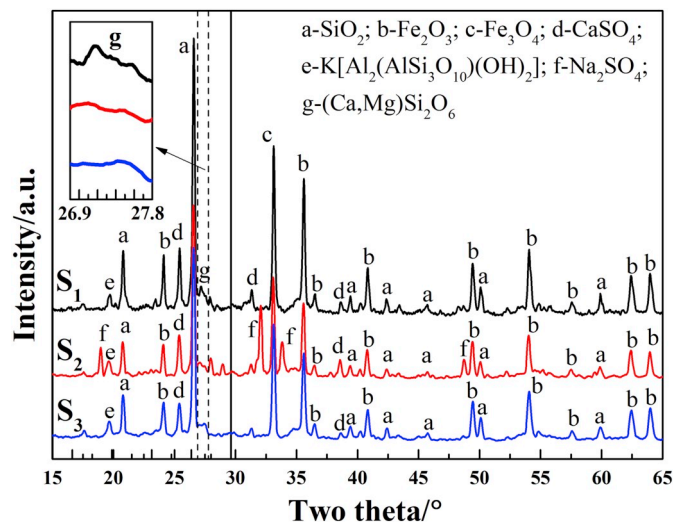
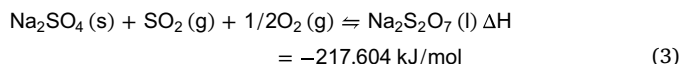
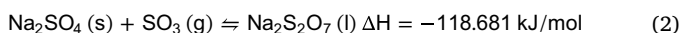
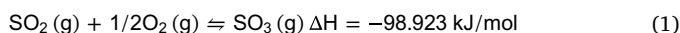


Fig. 4. XRD spectrograms for the calcines of S₁, S₂ and S₃. Conditions: the same as those shown in Fig. 3.

1988; Li et al., 2018; Lindberg et al., 2006; Shores and Fang, 1981). Na₂S₂O₇ has a low melting point of 387 °C (Lindberg et al., 2006). At 667 °C, Na₂S₂O₇ becomes unstable and decomposes to Na₂SO₄ and SO_x again.



For a gold ore containing a high content of S (20.76%) under the

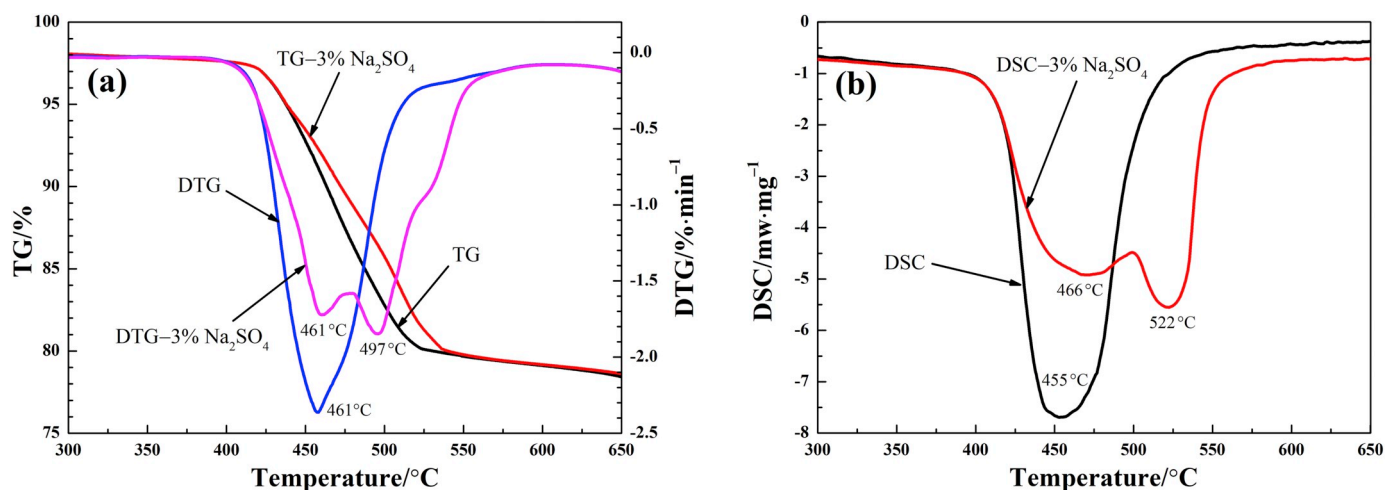


Fig. 5. (a) TG/DTG and (b) DSC curves of the gold ore in O_2 of 40% at a heating rate of $10\text{ }^\circ\text{C}/\text{min}$.

conditions of 40% of O_2 and $650\text{ }^\circ\text{C}$, besides SO_2 the gas of SO_3 can readily be formed from the roasting according to Eq. (1). In the presence of Na_2SO_4 , it is not unreasonable to expect it to react with SO_x and O_2 to form $Na_2S_2O_7$ (l) according to Eq. (2) or (3), resulting in a more serious sintering. Towards the end of the roasting, the decreasing concentration of SO_x due to its continuous removal would shift the equilibrium of Eq. (2) or (3) to the decomposition of $Na_2S_2O_7$ (l) back to Na_2SO_4 (s). In addition, a local high temperature higher than $667\text{ }^\circ\text{C}$ could easily occur during roasting that would lead to the decomposition of $Na_2S_2O_7$ (l) to Na_2SO_4 (s).

To further assess the sintering behaviour of the gold ore during roasting, TG–DTG–DSC analysis in O_2 of 40% is performed on the ore. The results are shown in Fig. 5.

Fig. 5(a) shows that, when the temperature increased from 300 to $650\text{ }^\circ\text{C}$, the rate of mass loss of the ore in the presence of Na_2SO_4 was slower than that without Na_2SO_4 . As discussed in our previous research (Liu et al., unpublished results, 2018), the mass loss of the ore mainly resulted from the oxidation and removal of S, As and C from the ore. Without Na_2SO_4 , DTG curve has a single significant peak at $\sim 461\text{ }^\circ\text{C}$; with Na_2SO_4 , an additional peak appeared at $\sim 497\text{ }^\circ\text{C}$ and the peaks have much reduced intensities. The DSC curves from the same

measurements are presented in Fig. 5(b), displaying the corresponding heat release pattern and intensity from the roasting. Similar to the mass loss, the addition of Na_2SO_4 has also changed the heat release from the roasting reactions from a single peak at $\sim 455\text{ }^\circ\text{C}$ to two peaks at $\sim 466\text{ }^\circ\text{C}$ and $\sim 522\text{ }^\circ\text{C}$ at a reduced intensity.

Even though the exact details of the reactions are difficult to determine and are not available at this stage, it is certain that the presence of Na_2SO_4 has changed the course of reaction that impacted the sintering and the outcome of the roasting process. Based on the result presented in Fig. 5, a possible mechanism for Na_2SO_4 assisted roasting of the gold ore is proposed and is depicted in Fig. 6. Soon after roasting started, $Na_2S_2O_7$ (l) was likely formed from the reaction of Na_2SO_4 with O_2 and the released SO_x during roasting. Among the solid ore and calcine particles, liquid $Na_2S_2O_7$ was like a binder, causing agglomeration and encapsulating some unreacted ore particles. This would reduce the gas diffusion and roasting reactions. Towards the end of the roasting, the decreasing SO_x concentration in the atmosphere because of its continuous removal caused the formed $Na_2S_2O_7$ (l) to decompose back to Na_2SO_4 and release SO_x , exposing the encapsulated ore particles again for their subsequent roasting. Due to the interconversion between Na_2SO_4 and $Na_2S_2O_7$ (l) during roasting, the exothermic effect was

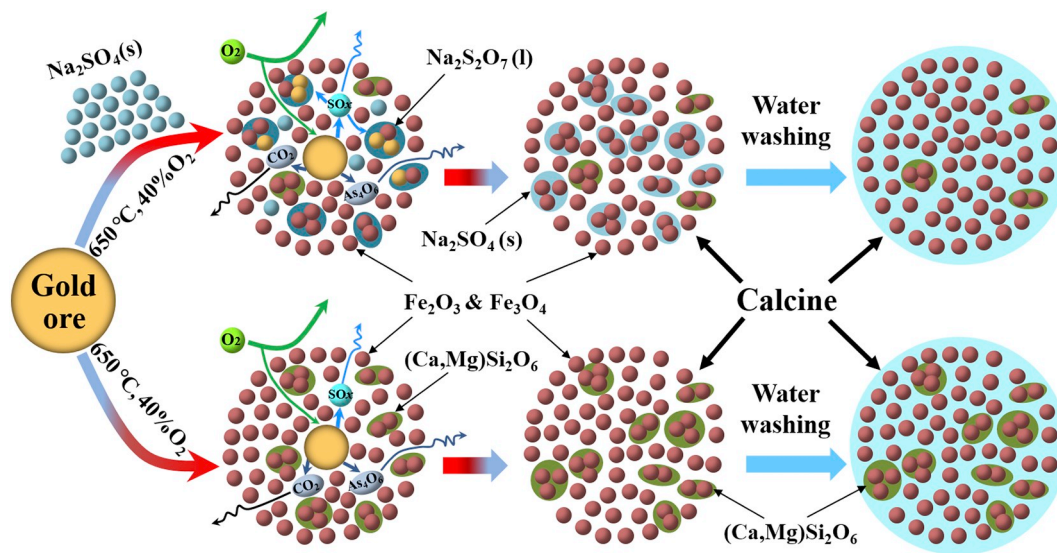


Fig. 6. The schematic diagram of the mechanism of Na_2SO_4 assisted roasting.

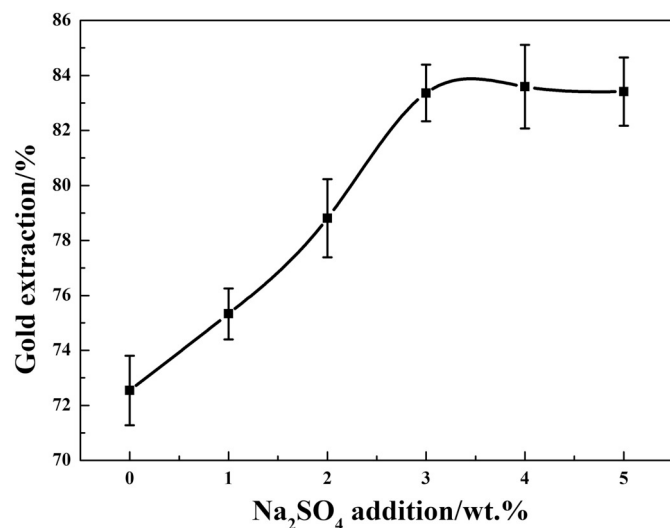


Fig. 7. Gold recovery with Na₂SO₄ addition in roasting.

much buffed compared with the roasting without Na₂SO₄. This likely resulted in the substantial reduction in the normal sintering phase, i.e., (Ca,Mg)Si₂O₆. When the roasting was complete, the sintering and agglomeration of the calcine were caused mainly by the binder Na₂SO₄ instead of (Ca,Mg)Si₂O₆. With the dissolution of water-soluble binder Na₂SO₄ through water washing, the sintering and agglomeration was significantly reduced. The interchange between Na₂S₂O₇ (I) and Na₂SO₄ during roasting also resulted in a more porous calcine that benefits its subsequent gold leaching.

4.1.2. Impact on gold recovery

The gold recovery from the calcines with different additions of Na₂SO₄ during roasting is shown in Fig. 7. It can be seen that the recovery rose with an increasing amount of Na₂SO₄ and reached a maximum of 83.4% at 3 wt% Na₂SO₄. Beyond that point, the gold recovery remained effectively the same. This is likely that 3 wt% Na₂SO₄ was sufficient to completely eliminate sintering and agglomeration during roasting, and their effects on gold recovery.

4.2. Removal of Sb

4.2.1. Sb in calcine and its speciation in an aqueous solution

As mentioned before, the existence of Sb in calcine is detrimental to gold recovery. Chemical analysis results on the calcine from the O₂-enriched single stage roasting with 3 wt% Na₂SO₄ show that it still has a residual content of Sb of 1.13%, as shown in Table 5. The chemical phases of Sb are listed in Table 6, which shows that Sb existed in the calcine mainly as oxide (65.49%), i.e., Sb₂O₃ and/or Sb₂O₄, and sulphide (31.5%), i.e., Sb₂S₃.

The level of Sb in the calcine is too high and needs to be removed before the extraction for gold. A feasible approach for Sb removal from the calcine is by selective leaching. The predominance areas of Sb species in an aqueous solution, based on thermodynamic analyses, are shown in an Eh–pH diagram in Fig. 8. It shows that, in the high pH

Table 5
Chemical composition of the calcine/(wt%).

Au ^a	SiO ₂	CaO	MgO	As	Fe	S	Sb	Al ₂ O ₃	C	K ₂ O
22.60	34.71	5.28	7.43	0.38	24.64	0.45	1.13	2.51	0.13	2.54

^a Unit g/t.

Table 6
Chemical phase of Sb in the calcine/(wt%).

Phase	Antimony oxide	Antimony sulphide	Antimony sulphate	Total
Content	0.740	0.356	0.034	1.13
Distribution	65.49	31.50	3.01	100.00

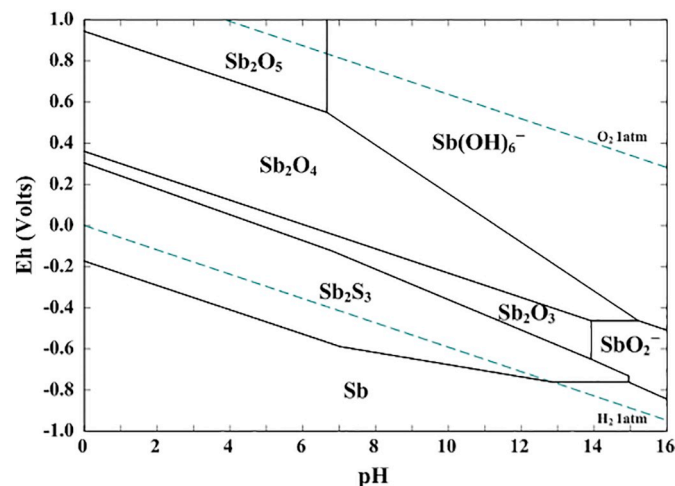
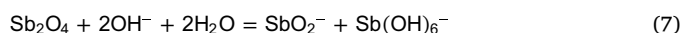
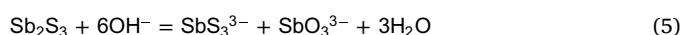


Fig. 8. Eh–pH diagram of Sb–S–H₂O system at 25 °C and 1 atm. Conditions: [Sb] 0.031 M (calculated according to Sb content in the calcine), [S²⁻] 0.064 M (i.e., 5 g/L Na₂S).

regions, the Sb species are soluble in the solution in the form of Sb(OH)₆⁻ and/or SbO₂⁻. This is confirmed in the speciation diagram (Fig. 9) that, in the Eh range of 0 V (Fig. 9(a)) to –0.25 V (Fig. 9(b)), the Sb species is mainly Sb(OH)₆⁻ with a small fraction of SbO₂⁻ under the alkaline conditions (pH > ~13).

Sb₂S₃ and Sb₂O₃ have been found to dissolve in alkaline sulphide solutions according to Eqs. (4)–(6) (Awe and Sandström, 2010; Celep et al., 2011; Gök, 2014; Li et al., 2019; Raschman and Sminčáková, 2012; Ubaldini et al., 2000), which are in agreement with the above thermodynamic analysis. In addition, thermodynamic analysis also suggests that Sb₂O₄ is soluble in alkaline solutions according to Eq. (7). Therefore, it is expected that Sb can be removed from the calcine through alkaline sulphide leaching.



4.2.2. Gold recovery after alkaline Na₂S leaching

Sb removal and gold recovery via alkaline Na₂S leaching of the calcine under different conditions are shown in Table 7. It shows that if the calcine is leached in a solution containing only NaOH (20 g/L), the content of Sb in the residue was reduced from 1.13% to 0.52% while the gold extraction from the residue increased from 83.4% to 88.2%. With the addition of only 5 g/L Na₂S to the alkaline, the Sb content was reduced to 0.15% and the gold recovery increased to 95.8%. A further increase of Na₂S would only have a slight enhancement on both the Sb removal and gold recovery.

To establish the mechanism by which Sb influences the gold extraction, size distribution and specific surface area of the calcine and

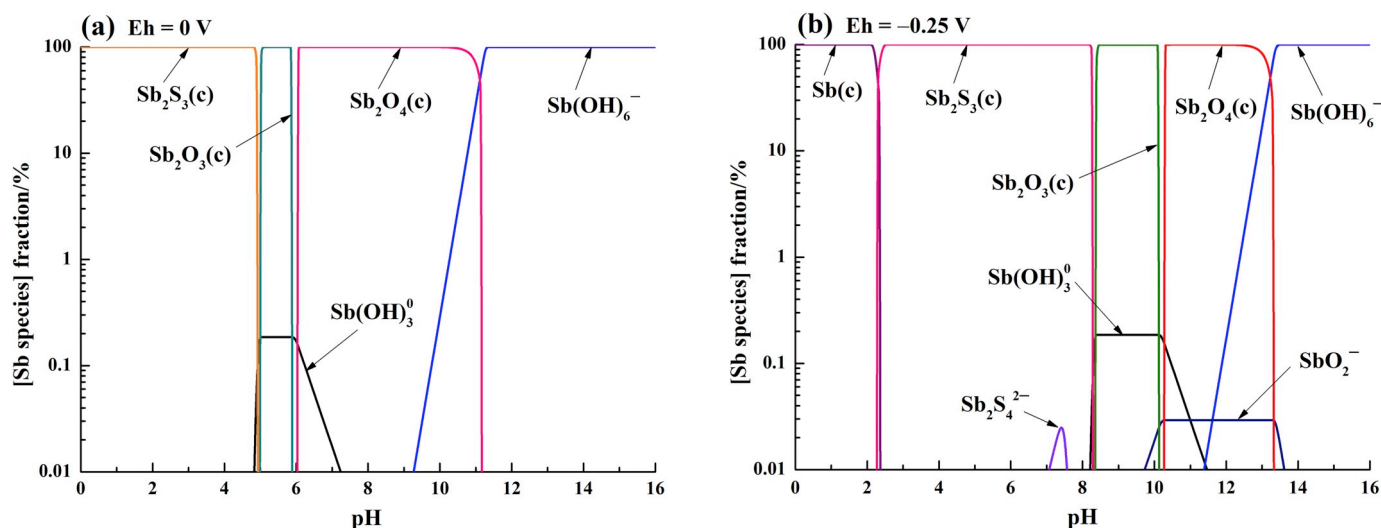


Fig. 9. Speciation of Sb species at 25 °C and 1 atm. Conditions: [Sb] 0.031 M, [S²⁻] 0.064 M; (a) Eh = 0 V, (b) Eh = -0.25 V.

Table 7
Gold extraction from the calcine treated by alkaline Na₂S leaching.

Alkaline Na ₂ S solution		T/°C	Time/h	Residual Sb content/%	Gold recovery/%
NaOH/(g/L)	Na ₂ S/(g/L)				
0	0	80	1	1.13	83.4
20	0	80	1	0.52	88.2
20	5	80	1	0.15	95.8
20	15	80	1	0.14	96.0

residue particles after Na₂S leaching were measured. The results are listed in Table 8. It can be seen that, although there is little change in the particle size of the calcine, there is a significant specific surface area increase from 6755 cm²/g to 7856 cm²/g, indicating that the calcine became more porous after the removal of Sb. This suggests that the increase in gold recovery is largely due to the improved exposure of gold particles from the Sb removal during cyanidation.

The effects of direct alkaline Na₂S leaching of the concentrate, O₂-enriched single stage roasting without or with Na₂SO₄, and Na₂S leaching after roasting with Na₂SO₄ on gold recovery were also compared, as shown in Fig. 10. It can be seen that, without any pre-treatment, the gold recovery from direct cyanidation of the concentrate was only 12%. Alkaline Na₂S leaching pre-treatment of the concentrate improved the gold recovery to 15.6%. O₂-enriched roasting with Na₂SO₄, without the alkaline Na₂S leaching step, then significantly increased the gold recovery to 83.4%. Addition of the alkaline Na₂S leaching step after the roasting further increased the gold recovery to

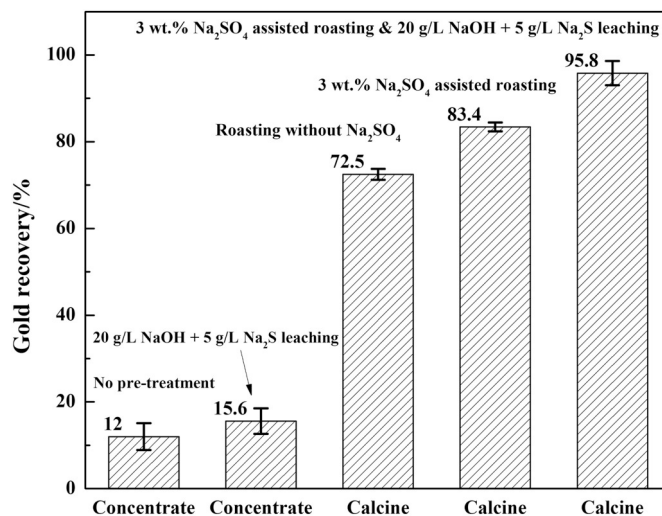


Fig. 10. Gold recoveries from concentrates and calcines.

95.8%. In other words, the gold recovery has progressively improved after each additional proposed pre-treatment.

In this investigation, a gold recovery of over 95% is achieved from a refractory gold ore through the addition of Na₂SO₄ to the optimised oxygen-enriched single stage roasting and an addition of an alkaline Na₂S leaching. While an extra processing step of alkaline Na₂S leaching will increase the production costs, this is justified from the improvement of gold recovery by nearly 12%. Based on this outcome, a process

Table 8
Size distribution and specific surface area of the calcine before and after alkaline Na₂S leaching under the optimal conditions.

Samples	Size distribution/(wt%)						Specific surface area/(cm ² /g)
	+ 74 μm	45–74 μm	37–45 μm	25–37 μm	– 25 μm	Total	
Calcine	4.15	16.52	9.05	13.82	56.46	100	6755
Residue	4.55	17.34	9.43	14.23	54.45	100	7856

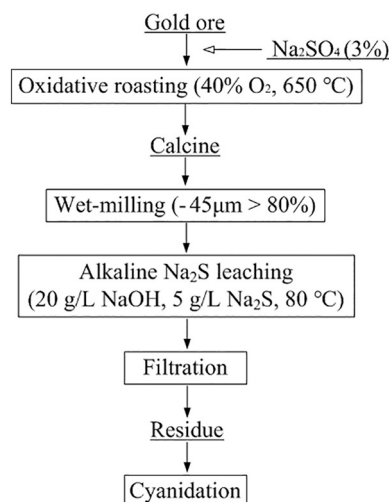


Fig. 11. Process flowsheet of extracting gold from refractory gold ores.

flowsheet shown in Fig. 11 is recommended for the processing of this type of refractory gold ores.

5. Conclusions

To further improve the gold recovery from a refractory ore, Na_2SO_4 is added in roasting to minimise sintering and alkaline Na_2S leaching utilised to remove Sb. Analytical results on physicochemical properties

of the calcines suggest that, compared to roasting without Na_2SO_4 , the formation of sintering phase, i.e., $(\text{Ca},\text{Mg})\text{Si}_2\text{O}_6$ was much reduced and the structure of washed calcine was more porous. The beneficial effect of Na_2SO_4 possibly lies in the interconversion between Na_2SO_4 and $\text{Na}_2\text{S}_2\text{O}_7$ occurring during roasting, which not only reduces the exothermic effect but also results in the formation of a water soluble phase. Gold leaching results showed that an optimised Na_2SO_4 assisted roasting could improve the gold recovery from 72.5% to 83.4%.

The presence of Sb in the calcine has been proven to be detrimental to the extraction of gold. Eh–pH and speciation diagrams of Sb species constructed from thermodynamic analyses suggest that the Sb oxide and sulphide can readily dissolve in alkaline solutions. Alkaline Na_2S leaching is shown to have effectively removed the Sb and made the calcine much more porous. This has significantly improved the exposure of gold particles in the calcine and consequently the gold recovery to reach over 95%.

Based on the outcome of this investigation, a process flow-chart is suggested for the processing of refractory gold ores that contain As, S, C and Sb.

Acknowledgements

Financial supports from the National Natural Science Foundation of China (Grant Nos. 51574284 and 51504293), the Fundamental Research Funds for the Central Universities of Central South University (No. 2017zzts194) and the China Scholarship Council (Grant Nos. 201706370222 and 201606370128) are all gratefully acknowledged.

Appendix A. Free energies of formation (kcal/mol) for relevant species^a

Species	ΔG_{298}° (kcal/mol)	Species	ΔG_{298}° (kcal/mol)	Species	ΔG_{298}° (kcal/mol)
S	0	SO_3^{2-} (a)	−116.287	Sb_2O_5	−203.380
H_2S (a)	−6.607	SO_4^{2-} (a)	−177.907	Sb_4O_6	−298.624
HS^- (a)	2.973	$\text{S}_2\text{O}_3^{2-}$ (a)	−124.825	Sb_2S_3	−48.626
H_2SO_3 (a)	−128.552	$\text{S}_2\text{O}_4^{2-}$ (a)	−143.539	$\text{Sb}_2(\text{SO}_4)_3$	−493.906
$\text{H}_2\text{S}_2\text{O}_3$ (a)	−128.006	$\text{S}_2\text{O}_6^{2-}$ (a)	−231.605	HSbO_2^- (a)	−97.391
$\text{H}_2\text{S}_2\text{O}_4$ (a)	−147.385	$\text{S}_2\text{O}_8^{2-}$ (a)	−266.460	SbO_2^- (a)	−82.383
HSO_3^- (a)	−126.103	$\text{S}_3\text{O}_6^{2-}$ (a)	−228.814	$\text{Sb}(\text{OH})_2^+$ (a) ^b	−99.313
HSO_4^- (a)	−180.524	$\text{S}_4\text{O}_6^{2-}$ (a)	−248.626	$\text{Sb}(\text{OH})_3^0$ (a)	−154.068
HS_2O_3^- (a)	−127.183	$\text{S}_5\text{O}_6^{2-}$ (a)	−228.331	$\text{Sb}(\text{OH})_4^-$ (a)	−194.326
HS_2O_4^- (a)	−146.862	H^+ (a)	0	$\text{Sb}(\text{OH})_5^0$ (a) ^b	−235.959
S^{2-} (a)	20.548	OH^- (a)	−37.577	$\text{Sb}(\text{OH})_6^-$ (a) ^b	−288.918
S_2^{2-} (a)	19.055	O_2 (a)	3.899	$\text{Sb}_{12}(\text{OH})_{64}^{4-}$ (a) ^b	−3085.918
S_3^{2-} (a)	17.657	H_2O (a)	−56.678	$\text{Sb}_{12}(\text{OH})_{65}^{5-}$ (a) ^b	−3137.650
S_4^{2-} (a)	16.589	Sb	0	$\text{Sb}_{12}(\text{OH})_{66}^{6-}$ (a) ^b	−3187.731
S_5^{2-} (a)	15.821	Sb_2O_3	−150.187	$\text{Sb}_{12}(\text{OH})_{67}^{7-}$ (a) ^b	−3236.462
S_6^{2-} (a)	15.827	Sb_2O_4	−190.223	$\text{Sb}_2\text{S}_4^{2-}$ (a)	−23.732

^a Data from the HSC Database (Roine, 2006).

^b ΔG_{298}° values were calculated using equation of $\Delta G_r^\circ = -RT \ln K = \sum(\nu_i \Delta G_f^\circ(i))$, of which log K values are from the hydrochemical log K database of Medusa-Hydra chemical equilibrium software (Puigdomenech, 2004).

References

- Awe, S.A., Sandström, Å., 2010. Selective leaching of arsenic and antimony from a tetrahedrite rich complex sulphide concentrate using alkaline sulphide solution. *Miner. Eng.* 23 (15), 1227–1236.
- Baláz, P., Achimovičová, M., 2006. Mechano-chemical leaching in hydrometallurgy of complex sulphides. *Hydrometallurgy* 84 (1–2), 60–68.
- Baláz, P., Achimovičová, M., Bastl, Z., Ohtani, T., Sánchez, M., 2000. Influence of mechanical activation on the alkaline leaching of enargite concentrate. *Hydrometallurgy* 54 (2–3), 205–216.
- Celep, O., Alp, I., Deveci, H., 2011. Improved gold and silver extraction from a refractory antimony ore by pretreatment with alkaline sulphide leach. *Hydrometallurgy* 105 (3), 234–239.
- Eriksson, G., 1979. An algorithm for the computation of aqueous multi-component, multiphase equilibria. *Anal. Chim. Acta* 112 (4), 375–383.
- Gök, Ö., 2014. Catalytic production of antimonate through alkaline leaching of stibnite concentrate. *Hydrometallurgy* 149 (13), 23–30.
- Guo, X., Li, D., Park, K.H., Tian, Q., Wu, Z., 2009. Leaching behavior of metals from a limonitic nickel laterite using a sulfation–roasting–leaching process. *Hydrometallurgy* 99 (3–4), 144–150.
- Haug, H.-H., 1989. Construction of Eh–pH and other stability diagrams of uranium in a multicomponent system with a microcomputer—II. Distribution diagrams. *Can. Metall. Q.* 28 (3), 235–239.
- Haug, H.-H., Cuentas, L., 1989. Construction of Eh–pH and other stability diagrams of uranium in a multicomponent system with a microcomputer—I. Domains of predominance diagrams. *Can. Metall. Q.* 28 (3), 225–234.
- King, R.B., 2005. *Encyclopedia of Inorganic Chemistry*, second ed. Wiley, Hoboken, New Jersey, United States.
- Kyle, J.H., Breuer, P.L., Bunney, K.G., Pleyzier, R., 2012. Review of trace toxic elements (Pb, Cd, Hg, As, Sb, Bi, Se, Te) and their deportment in gold processing. *Hydrometallurgy* 111–112 (3), 10–21.
- Lam, R.K.-F., 1988. Reactions of Na_2SO_4 (l) and $\text{CoSO}_4 \cdot \text{Na}_2\text{SO}_4$ (l) with SO_3 (g) and Al_2O_3 (s). Massachusetts Institute of Technology, Cambridge, Massachusetts, United States.

- States, pp. 900–1250 (K. Ph.D. Thesis).
- Li, Y., Liu, Z., Li, Q., Zhao, Z., Liu, Z., Zeng, L., 2011. Removal of arsenic from Waelz zinc oxide using a mixed NaOH–Na₂S leach. *Hydrometallurgy* 108 (3–4), 165–170.
- Li, Q., Ji, F., Xu, B., Hu, J., Yang, Y., Jiang, T., 2017. The consolidation mechanism of gold concentrates containing sulfur and carbon at oxygen-enriched air roasting. *Int. J. Miner. Metall. Mater.* 24 (4), 386–392.
- Li, G., Cheng, H., Chen, S., Lu, X., Xu, Q., Lu, C., 2018. Mechanism of Na₂SO₄ promoting nickel extraction from sulfide concentrates by sulfation roasting–water leaching. *Metall. Mater. Trans. B Process Metall. Mater. Process. Sci.* 49 (3), 1136–1148.
- Li, Y., Min, X., Ke, Y., Liu, D., Tang, C., 2019. Preparation of red mud-based geopolymer materials from MSWI fly ash and red mud by mechanical activation. *Waste Manag.* 83, 202–208.
- Lindberg, D., Backman, R., Chartrand, P., 2006. Thermodynamic evaluation and optimization of the (Na₂SO₄ + K₂SO₄ + Na₂S₂O₇ + K₂S₂O₇) system. *J. Chem. Thermodyn.* 38, 1568–1583.
- Liu, X., Li, Q., Zhang, Y., Jiang, T., Yang, Y., Xu, B., He, Y., 2018. Simultaneous removal of S and As from a refractory gold ore in a single stage O₂-enriched roasting process. *Metall. Mater. Trans. B Process Metall. Mater. Process. Sci.* (unpublished results).
- Liu, D., Min, X., Ke, Y., Chai, L., Liang, Y., Li, Y., Yao, L., Wang, Z., 2018. Co-treatment of flotation waste, neutralization sludge, and arsenic-containing gypsum sludge from copper smelting: solidification/stabilization of arsenic and heavy metals with minimal cement clinker. *Environ. Sci. Pollut. Res.* 25 (8), 7600–7607.
- Padilla, R., Ramírez, G., Ruiz, M.C., 2010. High-temperature volatilization mechanism of stibnite in nitrogen-oxygen atmospheres. *Metall. Mater. Trans. B Process Metall. Mater. Process. Sci.* 41 (6), 1284–1292.
- Padilla, R., Aracena, A., Ruiz, M.C., 2014. Kinetics of stibnite (Sb₂S₃) oxidation at roasting temperatures. *J. Min. Metall. B* 50 (2), 127–132.
- Prasad, S., Pandey, B.D., 1998. Alternative processes for treatment of chalcopyrite—a review. *Miner. Eng.* 11 (8), 763–781.
- Puigdomenech, I., 2004. MEDUSA: Make Equilibrium Diagrams Using Sophisticated Algorithms. Royal Institute of Technology, Stockholm, Sweden.
- Rao, K.A., Natarajan, R., Padmanabhan, N.P.H., 2001. Studies on recovery of copper, nickel, cobalt and molybdenum values from a bulk sulphide concentrate of an Indian uranium ore. *Hydrometallurgy* 62 (2), 115–124.
- Raschman, P., Sminčáková, E., 2012. Kinetics of leaching of stibnite by mixed Na₂S and NaOH solutions. *Hydrometallurgy* 113–114 (3), 60–66.
- Roine, A., 2006. Outokumpu HSC Chemistry for Windows: chemical reaction and equilibrium software with extensive thermochemical database. In: User's Guide, Version 6.0. Outokumpu Research Oy, Pori, Finland.
- Shores, D.A., Fang, W.C., 1981. Transport of oxidant in molten Na₂SO₄ in O₂-SO₂-SO₃ environments. *J. Electrochem. Soc.* 128 (2), 346–348.
- Sminčáková, E., Raschman, P., 2011. Leaching of natural stibnite using Na₂S and NaOH solutions. *Int. J. Energ. Eng.* 1 (2), 85–89.
- Thomas, K.G., Cole, A.P., 2016. In: Adams, M.D. (Ed.), *Gold Ore Processing – Project Development and Operations*. vol. 23. pp. 373–392 Roasting developments—Especially oxygenated roasting.
- Ubal dini, S., Vegliò, F., Fornari, P., Abbruzzese, C., 2000. Process flow-sheet for gold and antimony recovery from stibnite. *Hydrometallurgy* 57 (3), 187–199.
- Xu, B., Yang, Y., Li, Q., Jiang, T., Liu, S., Li, G., 2016. The development of an environmentally friendly leaching process of a high C, As and Sb bearing sulfide gold concentrate. *Miner. Eng.* 89, 138–147.
- Zeng, W., Wang, S., Free, M.L., Tang, C., Xiao, R., Liang, Y., 2018. Design and modeling of an innovative copper electrolytic cell. *J. Electrochem. Soc.* 165 (14), E798–E807.
- Živkovića, Ž., Štrbaca, N., Živkovića, D., Grujičića, D., Boyanovb, B., 2002. Kinetics and mechanism of Sb₂S₃ oxidation process. *Thermochim. Acta* 383 (1–2), 137–143.